Precipitation mode and kinetics of Laves phase on a eutectoid type reaction (δ→ γ+Laves) in high Cr ferritic alloys

Zhetao Yuan[1], Mikael Perrut[2] and Satoru Kobayashi[1]

[1]*Department of Materials Science & Technology, Tokyo Institute of Technology, 2-12-1 Ookayama, Meguro-ku, Tokyo, 152-8550 Japan.*
[2]*Department of Materials and Structures, ONERA - The French Aerospace Lab, 29, avenue de la Division Leclerc Châtillon, 92320 France.*

The formation of periodically arrayed rows of fine Fe_2Hf Laves phase particles was found to occur by interphase precipitation on a eutectoid type reaction path: δ-Fe → γ-Fe +Laves in 9Cr ferritic alloys with a small addition of Hf. In the present work, the precipitate morphology and precipitation mode of Laves phase were investigated on the eutectoid path in Ta doped high Cr ferritic alloys. The precipitation mode was found to change from fibrous precipitation to interphase precipitation with raising the δ→ γ transformation kinetics. The observed transition in precipitation mode was discussed in terms of the balance between the diffusion rate of the solute element and the velocity of migrating δ/γ interface.

Keywords: *interphase precipitation; eutectoid reaction; heat resistant 9 chromium ferritic steels*

1. Introduction

Heat resistant 9Cr ferritic steels are an important class of materals for high temperature components such as pipes, tubing, and turbines in thermal power generation systems due to their low thermal expansion coefficient, high thermal conductivity, and relatively low cost [1, 2]. The 9Cr ferritic steels are heat-treated to form a tempered lath martensitic structure strengthened with $M_{23}C_6$ type carbide (M: Cr, Fe, Mo) and (V, Nb)(C, N) carbonitride particles against dislocation motion, recovery, and recrystallization. Such strengthening particles are, however, prone to particle coarsening and decomposition, which are considered to trigger the degradation of creep strength of the materials at long-term conditions [1, 2]. Due to the limitation of the stability of carbide and carbonitride particles at high temperatures, a new strategy is required to develop heat resistant ferritic steels using particles with improved high temperature stability.

Laves phase, A_2B type intermetallic phase, is expected to show better high temperature stability and many types of Fe based Laves phases are available. In the flamework of finding a candidate for strengthening high Cr ferritic steels, the formation of periodically arrayed rows of fine Fe_2Hf Laves phase particles was found to occur in a 9 wt. % Cr based ferrite alloy [3-8]. The studies have revealed that the fine Fe_2Hf particles were formed through interphase precipitation (hereafter designated as IPP) on migrating δ/γ interfaces along a eutectoid type reaction path: δ-ferrite → γ-austenite + Fe_2Hf-Laves, which is followed by a γ to α-ferrite transformation. This finding allows us to expect develop a new type of heat resistant ferritic steel strengthened with the intermetallic phase using a eutectoid-type precipitation route.

The same eutectoid-type reaction path: δ→ γ+Laves phase is available in the Fe-Ta and the Fe-Nb binary alloy systems [9]. Our preliminary experiments in Cr doped ternary Fe-Cr-Ta alloys revealed that Fe_2Ta type Laves phase was formed with fibrous morphology along the eutectoid reaction path. The formation of fibrous Laves phase, called "fibrous precipitation" [10], is hereafter designated as FP, was found to occur by more than three orders of magnitude slower than IPP observed in Fe-Cr-Hf ternary alloys with similar Cr contents. We also found that a transition from FP to IPP took place when the δ→γ transformation kinetics was raised by lowering the Cr content in Fe-Cr-Ta alloys in our recent study [11].

In the present abstract, we briefly explain how the precipitate morphology and mode of Fe_2Ta Laves phase change with raising the δ→γ transformation kinetics in Fe-Cr-Ta ternary alloys and discuss the transition in the two precipitation modes (FP vs. IPP).

2. Experimental Procedure

Table 1 lists the chemical compositions of the alloys studied. The chemical compositions are given in atomic percent through this paper. The alloys are a series of Fe-Cr-Ta alloys with different Cr concentration and a fixed eutectoid Ta concentration. Changing Cr concentration will allow vary the δ→ γ transformation rate (i.e. the migration velocity of δ/γ interphase boundary) with little change in the precipitation rate of Laves phase.

Table 1 Chemical compositions and designations of the studied alloys

Alloy designation	Chemical composition (at.%)			
	Fe	Cr	Hf	Ta
Fe-7.5Cr-0.6Ta	bal.	7.5	-	0.65
Fe-7.7Cr-0.6Ta	bal.	7.7	-	0.65
Fe-8.1Cr-0.6Ta	bal.	8.1	-	0.65
Fe-8.5Cr-0.6Ta	bal.	8.5	-	0.65
Fe-9.5Cr-0.6Ta	bal.	9.5	-	0.62

The arc-melted alloys were fabricated to cylinders of 3 mm in diameter and 10 mm in length with a hole drilled along the longitudinal direction of the cylinder in the depth of 5 mm. The cylindrical specimens were solutionized at 1250 °C in their δ single-phase region for a period of 5 min, then directly cooled to isothermally aged temperatures in the γ+Fe_2Ta two-phase region, hold for certain periods of

time, and finally gas cooled. During the heat treatments, the temperature profiles were tracked using an R-type thermocouple which was inserted in the hole of the specimen. The cooling rate from the solution temperature to the isothermal aging temperature was about 35 °C/s.

Heat-treated specimens were sectioned and the cross sections were prepared by grinding, mechanically polishing down to 1 μm Al_2O_3 polishing suspension, and chemical polishing with SiO_2 polishing suspension. Microstructures were observed with an optical microscope (OM) and a field emission scanning electron microscope (FE-SEM) with backscattered electron (BSE) detector.

3. Results and discussion

3.1 Measurement of δ/γ interface velocity

The δ→ γ transformation occurred at the surface of the specimens and δ grain boundaries during heat treatments [11]. The velocity of the δ/γ interface migration was estimated at both γ nucleating sites by measuring the width of the fine-grained areas. Figure 1 shows the estimated interface velocity as a function of temperature for Ta doped alloys with different Cr contents and Hf doped alloys [11]. The estimated velocity shows an inverse C shape. The velocity for the Fe-9.5Cr-0.6Ta alloy is ~3 orders of magnitude as slow as that for the Hf doped alloys with similar Cr contents. The velocity in the Ta doped alloys are found to increase with decreasing the Cr content from 9.5% to 8.5% by one order of magnitude, and from 8.5% to 8.0% by another one order of magnitude.

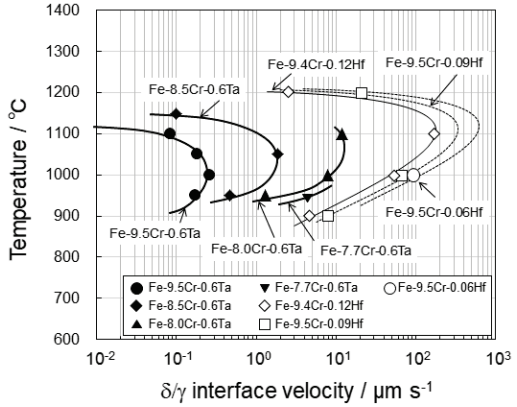

Fig. 1 The δ/γ interface velocity measured at aged temperatures in Ta doped and Hf doped alloys [11].

3.2 Precipitation mode and morphology vs. δ/γ interface velocity

The precipitation mode and precipitate morphology changed with raising the δ/γ interface velocity. The precipitation mode was identified as FP at a relatively slow δ/γ interface velocity range according to the facts that the precipitates are fibrous, and their longitudinal direction is oriented perpendicular to the δ/γ interface. At relatively higher δ/γ interface velocity, a microstructure formed by IPP was found, where periodical arrays of fine particles are arranged parallel to the advancing δ/γ interface [11]. Figure 2 shows some examples of micrographs taken from Ta doped alloys with the transition δ/γ migrating velocity. Two types of morphologies were found to form at this condition. It was also recognized that the fibers are often fragmented.

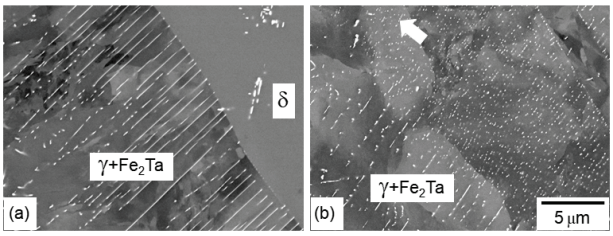

Fig. 2 Backscattered electron images of Ta doped alloys heat-treated at δ phase field and subsequently aged at 950°C for 5min in Fe-8.5Cr-0.6Ta alloy showing the occurrence of: (a) FP and (b) IPP. The arrow in (b) indicates the migration direction of the δ/γ interface.

3.3 Transition between the precipitation modes

The precipitation mode on the eutectoid type reaction path: δ→ γ+Fe_2Ta was observed to change from FP to IPP with increasing the δ/γ interface velocity at a critical velocity of 0.2~1 μm/s. The observed transition between the precipitation modes is discussed below in terms of available theoretical treatments on the growth of eutectoid product phases.

It is generally considered that fibrous precipitation occurs on eutectoid reactions when the precipitate phase can grow in a cooperative manner with the other product phase in the reaction. The precipitate phase corresponds to the Laves phase and the other product phase to the γ phase in the present case. The growth rate treatments through volume diffusion or boundary diffusion of solute elements were adopted for the fibrous aggregates observed in the present study. By referring [12, 13], the volume diffusion-based growth rate v_v of the present case is given by the following equation:

$$v_v = D_V^{\delta}/(f^{\gamma} f^{Fe2Ta} S)(x^{\delta/\gamma} - x^{\delta/Fe2Ta})/(x_e^{Fe2Ta/\gamma} - x_e^{\gamma/Fe2Ta})$$

where D_V^{δ} is volume diffusion coefficient of solute element (Ta) in the δ phase, f is the volume fraction of each phase, S is interlamellar (inter-fiber) spacing. $x^{\delta/\gamma}$ and $x^{\delta/Fe2Ta}$ is the solute content (in mole fraction) in the δ phase in front of the eutectoid γ phase and Fe_2Ta phase, respectively. $x_e^{Fe2Ta/\gamma}$ and $x_e^{\gamma/Fe2Ta}$ is the equilibrium solute content in the Fe_2Ta and the γ phase, respectively. The boundary diffusion-based growth rate v_B is given by the following equation:

$$v_B = 8\, k\, w D_B/(3 f^{\gamma} f^{Fe2Ta} S^2)(x^{\delta/\gamma} - x^{\delta/Fe2Ta})/(x_e^{Fe2Ta/\gamma} - x_e^{\gamma/Fe2Ta})$$

where w is the width of advancing δ/γ interface, D_B is boundary diffusion coefficient, and k is defined as the distribution coefficient for the solute element between the δ/γ interface and the initial parent δ phase. Both types of growth rates were calculated using the measured inter-fiber spacing, reported diffusion coefficient values [14, 15], and the volume fractions and the solute contents which were estimated from our phase diagram study on the Fe-Cr-Ta ternary system [8], ignoring the molar volume difference among the constituent phases. The specific δD_B value for Ta at ferrite/austenite boundary was not available, so that the reported value for grain boundary diffusion of Fe in pure iron was taken, which would be reasonable since the value was reported to be independent of the diffusive

species (Fe, Ni, Co, and Cr) and of the matrix phases (ferrite or austenite) [15]. The calculated v values are summarized in Table 2 [11]. The value of 1 was taken for k since the values of $x^{\delta/\gamma}$ and $x^{\delta/Fe2Ta}$ are almost equally away from the bulk Ta content. The calculated growth rate values demonstrate that the growth rate which is achievable by boundary diffusion is 5 orders of magnitude higher than the rate by the volume diffusion.

Table 2 The calculated velocity of eutectoid fibrous growth in the Fe-8.5Cr-0.6Ta alloy based on the equations given in the manuscript and thermodynamic, diffusional and microstrucural parameters [11].

Temp. (°C)	1100	1050	1000	950
v_V (mm/s)	2.7×10^{-7}	1.9×10^{-7}	9.3×10^{-8}	3.9×10^{-8}
v_B (mm/s)	2.4×10^{-2}	3.8×10^{-2}	6.9×10^{-2}	3.9×10^{-2}

Our observations revealed that the fibrous Fe_2Ta precipitates are often fragmented, as mentioned above. The fragmented fibrous feature suggests that the advancing δ/γ interface moves at a rate just above the rate at which the precipitate can collect sufficient solute element to be continuously grown. Closer values between the measured δ/γ interface velocity range for FP and the calculated v_B rather than v_v indicate that the growth of fibrous precipitates is controlled by boundary diffusion of solute element through the advancing δ/γ interface. As the interface velocity increases, the time for the boundary diffusion becomes insufficient to supply the solute element to grow the fibers continuously, and then the fibers get more fragmented. The increased interface velocity may also allow the solute content to remain high at the δ/γ interface, and the supersaturated solute is used for the nucleation of IPP at the moving δ/γ interface, which is a possible scenario of the transition from FP to IPP which was observed in the present study.

4. Summary

The precipitate morphology and mode of Laves phase on a eutectoid type reaction path: δ-Fe → γ-Fe +Laves were investigated in Ta doped 9Cr ferritic alloys. The main results are:

(1) The precipitation mode was found to change from fibrous precipitation to interphase precipitation with raising the δ→ γ transformation kinetics.

(2) Semi-quantitative analysis suggests that the growth of fibrous precipitates is controlled by boundary diffusion of solute element through the advancing δ/γ interface rather than the volume diffusion in the parent phase. The transition would thus be related to the time availability for solute diffusion through the advancing interface boundary diffusion to grow the fibrous precipitates.

Acknowledgments

This study was financed by the ISIJ Research Promotion Grand, university research aid of JFE 21st Century Fundation, and JSPS KAKENHI Grand Number 15K06496.

References

1) F. Masuyama: ISIJ Int., 41(2001), 612.
2) K. Sawada, H. Kushima, M. Tabuchi and K. Kimura: Mater. Sci. Eng. A, 528(2011), 5511.
3) S. Kobayashi, K. Kimura and K. Tsuzaki: Intermetallics, 46(2014), 80.
4) S. Kobayashi: MRS Online Proc. Lib., 1760(2014), 217.
5) S. Kobayashi and T. Hibaru, ISIJ Int., 55(2015) 293–299.
6) Z. Yuan, S. Kobayashi, M. Takeyama, Proc. Jt. EPRI-123HiMAT Int. Conf. Adv. High-Temperature Mater., ASM International, Nagasaki, Japan, 2019: p. 90.
7) S. Kobayashi and T. Hara: Appl. Sci., 11(2021), 2327.
8) Z. Yuan and S. Kobayashi: Metals, 12(2022), 102.
9) U.R. Kattner and B.P. Burton, Phase diagrams of binary iron alloys, ASM International, Materials Park, OH, 1993.
10) D.A. Porter and K.E. Eastering: Phase Transformations in Metals and Alloys, 2nd ed.; Stanley Thornes Publishers Ltd.: Gloucestershire, UK, (1992), 349.
11) Z. Yuan, M. Perrut, and S. Kobayashi: ISIJ International, 63(2023), 1413.
12) H.I. Aaronson, M. Enomoto and J.K. Lee: Mechanisms of Diffusional Phase Transformations in Metals and Alloys; CRC Press: NW, 2010, 588.
13) M. Hillert: Metall. Trans., 3(1972), 2729. https://doi.org/10.1007/BF02652840
14) Q.A. Shaikh: Mater. Sci. Technol., 6(1990), 1177. https://doi.org/10.1179/mst.1990.6.12.1177
15) J. Fridberg, L-E. Törndahl and M. Hillert: Jernkond. Ann., 153(1969), 264.